Extending the method of characteristics to simulate rapid flooding of large and complex systems

S.C.Giuseppin
Dynaflow Research Group

ABSTRACT
Deluge fire water systems can be subjected to large fluid-induced forces during rapid filling. There is therefore an interest to assess beforehand whether such a system can withstand these forces. The use of CFD methods for rapid filling simulations is often not practical due to the size of the systems involved. The method of characteristics (MoC), on the other hand, is much more efficient but is originally limited to single-phase fluid flow. Although the literature describes several methods to extend the MoC to two-phase fluid flow, these methods tend to be applied to relatively simple piping systems. This paper therefore describes a method for extending the MoC to simulate rapid flooding of large piping systems with complex topologies. The method tracks the position of one or more gas volumes and calculates the back pressure of entrapped gas as it is released from the system. This paper will show that the presented method can simulate rapid flooding of large and complex systems in an efficient way. It will also show that the results obtained for simple piping configurations are in agreement with the literature, provided that the wave speed is adjusted to account for entrapped gas in the liquid phase.

Notation

A	cross-sectional flow area of pipe
A_{in}	projected inflow area
A_{out}	projected outflow area
c	wave speed in liquid phase
c_d	vent discharge coefficient
C_M, B_M	positive MoC coefficients
C_N, B_N	negative MoC coefficients
d	orifice diameter
$\boldsymbol{d}$	direction vector of linear momentum
D	inner pipe diameter
f	Darcy-Weisbach friction factor
f_a	air fraction
f_l	liquid fraction
g	gravitational acceleration
L_c	grid cell length
N_{in}	number of inflow pipe elements connected to junction
N_{out}	number of outflow pipe elements connected to junction
p	pressure in liquid phase
p_0	atmospheric gas pressure
p_P	pressure in liquid phase in grid point P
p_A, p_B	pressure in liquid phase in grid point A and B, respectively
p_g	pressure in gas phase
Q_i	rate of change of gas volume due to moving interfaces
Q_o	volumetric flow rate through vents
$\boldsymbol{r}$	direction vector of pipe element
t, t_0	time and time of previous time step

u	flow velocity of liquid phase
u_+, u_-	interface velocity for positive and negative interface, respectively
V	gas volume
α	pipe's angle of incline
γ	ratio of specific heats of the gas
Δt	time step size
ΔV	change in gas volume
Δx	grid cell length
ρ	density of liquid phase
ρ_0	atmospheric gas density
ϕ	mass flow rate of liquid phase
ϕ_{in}	absolute liquid mass flow rate that flows into a junction
ϕ_o	gas mass flow rate through vent
ϕ_P	mass flow rate of liquid phase in grid point P
ϕ_A, ϕ_B	mass flow rate of liquid phase in grid point A and B, respectively
ϕ_+, ϕ_-	mass flow rate at positive and negative interface, respectively

1 INTRODUCTION

Rapid filling occurs when a drained pipeline is suddenly flooded at a high enough flow rate that the liquid-gas interface is more or less perpendicular to the axis of the pipeline. The flooding liquid propagates at high velocities through the system. These high velocities result in significant unbalanced forces that can cause failures in the pipeline, such as pipe fractures or support breaks. The impact pressures due to rapid filling of a pipeline has been studied and several numerical models have been proposed to accurately predict the impact pressures; rigid-column models that assume the liquid-pipe system is incompressible (Lou et al. (1996)), elastic models that account for the elasticity of the liquid column (Malekpour et al. (2011); Zhou et al. (2011); Zhou et al. (2018)), and CFD models to resolve the multiphase flow in 3-D (Li et al. (2018)). In elastic models often a small part of the liquid column near the air interface, the plug, is assumed to behave as a rigid-column, this subset of elastic models is referred to as virtual-plug models. The different rapid filling models predict the initial (highest) impact pressure well.

The Method of Characteristics is a commonly used solution method to predict transients for engineering purposes in pipelines. However, the above-mentioned rapid filling models are either not suited for direct implementation in existing MoC routines, since they require significant changes to the data structures, or the models have significant performance overhead to obtain the accuracy required for academic purposes. Moreover, the mentioned papers describe situations of a single pipeline with an entrapped air volume that may or may not be expelled from an orifice. However, real pipeline systems tend to be much more complex with many branches to different outlets. For example, fire water systems often consist of a long pipeline from the pump/valve station and branches near the end to monitors, sprinklers, or other outlets. Each branch may eventually become a separate entrapped air volume. An efficient model is required to predict the rapid filling in reasonable computational time.

This paper proposes a model that minimizes the impact on existing MoC code. The model is based on a virtual plug method, but trades off accuracy for performance and code simplification. The result is a model that only acts as a post processing step in the MoC code. The proposed model allows for multiple pockets of gas to be present in the pipeline at any given moment. Each pocket may have multiple interfaces with

the liquid that floods the system. In order to optimize the volume tracking, pockets are defined as graphs, and the movement of interfaces expands or reduces the pockets graph. The graph topology is used to efficiently split pockets at junctions.
In the proposed model, gas volumes grow and shrink according to the relations of an isentropic process, and can take in or expel gas to the environment via vents. The gas properties, including the pressure, are assumed to be homogeneous throughout the volume and, therefore, the wave speed in the gas phase to be infinite. The liquid-gas interfaces are implemented such that only information of the grid cells containing the interfaces is required.
A cell containing a liquid-gas interface is considered to be fully filled for inertia and friction purposes. This is a more straightforward but less accurate approach than the one proposed by Zhou et al. (2018) and Malekpour et al. (2011). They model a small part of the liquid near the liquid-gas interface as rigid. This rigid part allows them to capture the increasing inertia and friction of the liquid column. However, their methods require the characteristic coefficients from the cells upstream of the cell that contains the interface and are defined by a more complex set of equations. The reduced accuracy is noticeable as small pressure surges, but does not significantly affect the overall results.

2 METHOD OF CHARACTERISTICS

The flow in the pipeline is assumed to be 1-D. The momentum and continuity equations can be written as

$$p_x + \frac{1}{A}\phi_t + f_l \rho g \sin\alpha + \frac{f}{2\rho D A^2}\phi|\phi| = 0 \quad (1)$$

$$p_t + \frac{c^2}{A}\phi_x = 0 \quad (2)$$

Here p is the pressure, ϕ is the mass flow rate, A is the flow area, f_l is the liquid fraction, ρ is the liquid density, g is the gravitational acceleration, α is the pipe's angle of incline, f is the Darcy-Weisbach friction factor, D is the pipe's bore, and c is the wave speed. The subscripts x and t are the partial and temporal derivatives, respectively. This system of equations can be solved using the method of characteristics (MoC).(6) In the MoC these partial differential equations are evaluated along the characteristic lines in the space-time domain. The pressure and flow rate are calculated at discrete locations in the space-time domain. Those locations will be referred to as the grid points and the space between two grid points will be referred to as grid cells.
The derivation of the solution will be omitted as it is described in many text books about differential equations or numerical pipe flow. The pressure and the flow rate at a grid point P along the positive characteristic follow the relation

$$p_P = C_M - B_M \phi_P \quad (3)$$

Here p_P and ϕ_P are the pressure and mass flow rate in grid point P, and C_M and B_M are the positive MoC coefficients. The pressure and the flow rate at a grid point P along the negative characteristic follow the relation

$$p_P = C_N - B_N \phi_P \quad (4)$$

Here C_N and B_N are MoC coefficients for the negative characteristic. The MoC coefficients C_M, C_N, B_M, and B_N are given by

$$C_M = p_A - g\rho\Delta x \sin\alpha + \frac{c}{A}\phi_A \quad 5$$

$$C_N = p_B + g\rho\Delta x \sin\alpha - \frac{c}{A}\phi_B \quad 6$$

$$B_M = \frac{c}{A} + \frac{f\Delta x}{2\rho DA^2}|\phi_A| \quad 7$$

$$B_N = \frac{c}{A} + \frac{f\Delta x}{2\rho DA^2}|\phi_B| \quad 8$$

Here Δx is the grid cell length, and the subscripts A and B denote the value of the previous time step for the upstream point and downstream point, respectively. Equations 3 and 4 are required to calculate the propagation velocity of a liquid-gas interface.
The wave speed depends on pipe materials and geometry. Therefore, the MoC requires the piping system to be discretized into pipe elements. A pipe element is a section of piping between two junctions that have the same wave speed.

3 NUMERICAL MODEL

The rapid filling model proposed here is based on the following: (1) flooding happens sufficiently fast such that the liquid-gas interfaces can be assumed to perfectly cover the cross-sectional area of a pipe; (2) the compression and expansion of the gas are isentropic processes; (3) transient effects within the gas volume are negligible; (4) fittings, like valves, have no effect on the state of the gas phase; (5) the gas-liquid interfaces propagate significantly slower that the speed of sound; (6) gas is not entrained in the liquid phase; (7) all air inlet/outlets operate at the same atmospheric pressure and temperature; and (8) a quasi-steady wall friction factor is sufficiently accurate. Note that the fourth assumption implies that the pressure and temperature within a gas volume is homogeneous and the speed of the sound infinite. The sixth assumption implies that the wave speed of the liquid does not change in time.

The geometry and size of a gas changes due to the movement of its interfaces with the liquid and due to expulsion (or in take) of gas through vents. The volume of a pocket can be determined by

$$V(t) = V(t_0) + \int_{t_0}^{t} Q_i(t)dt \quad 9$$

Here V is the size of the pocket, t is the current time and t_0 is a time in the past, and Q_i is the rate of change due to moving liquid-gas interfaces. It is assumed that the size of a gas volume is governed by the following isentropic relation

$$p_g V^{\gamma} = \text{constant} \quad 10$$

Here p_g is the gas pressure, and γ is the ratio of specific heats. Using the isentropic relation, the volume change due to vents is given by

$$\Delta V_0(t) = \int_{t_0}^{t} \left(\frac{p_g(t)}{p_g(t_0)}\right)^{\frac{1}{\gamma}} Q_o(t)dt \qquad 11$$

Here ΔV_0 is the expelled volume at $p_g(t_0)$, and Q_o is the volumetric flow through vents. According to the isentropic relation of equation 10, the equations 9 and 11 relate as

$$p_g(t)V(t)^\gamma = p_g(t_0)(V(t_0) - \Delta V_0(t))^\gamma \qquad 12$$

Here the left-hand side is the state at time t and the right-hand side is the state at time t_0. The model assumes that an interface is perpendicular to the pipeline axis, so that an interface always lies within a single grid cell.
The flow in the liquid phase and the movement of the liquid-gas interfaces is determined by means of the MoC. As a consequence, the model distinguishes between positive and negative interfaces. A positive interface has the liquid upstream and the gas downstream; its movement is determined by the positive MoC characteristic of the cell, equation 3, with the pocket's pressure as pressure. A negative interface has the liquid downstream and the gas upstream; its movement is determined by the negative MoC characteristic which is described in equation 4. This means that the movement of an interface depends on the inertia and friction associated with an entire grid cell, even though it is partially filled with liquid. This will cause small pressure perturbations when an interface moves between grid cells. However, it is expected that these perturbations do not significantly affect the overall transient flow conditions within the pipeline system.
Using the pocket's pressure as pressure in equations 3 and 4 shows that the mass flow rate at the interface is given by

$$\phi_+ = \frac{C_M - p_g}{B_M}, \qquad \phi_- = \frac{p_g - C_N}{B_N} \qquad 13$$

Here ϕ_+ and ϕ_- are the mass flow rates at the positive and negative interfaces, respectively. As the interfaces move with the same velocity as the liquid, the velocity of an interface is given by

$$u_+ = \frac{1}{\rho} A\phi_+, \qquad u_- = \frac{1}{\rho} A\phi_- \qquad 14$$

Under adiabatic conditions, the gas mass flow rate through vents to the atmosphere can be expressed by(10)

$$\phi_o = c_d A \sqrt{2p_0\rho_0 \frac{\gamma}{\gamma - 1}\left[\left(\frac{p_g}{p_0}\right)^{\frac{2}{\gamma}} - \left(\frac{p_g}{p_0}\right)^{\frac{\gamma+1}{\gamma}}\right]} \qquad 15$$

Here p_0 is the atmospheric pressure, ρ_0 is the gas density at atmospheric pressure, and c_d is the discharge coefficient of the vent. Note that c_d has been added to account for possible pressure losses. If p_g/p_0 is greater than a critical ratio, then the flow through the vent is choked and the mass flow rate is calculated as

$$\phi_o = c_d A \sqrt{\gamma p_0 \rho_0 \left(\frac{2}{\gamma+1}\right)^{\frac{\gamma+1}{\gamma-1}}} \tag{16}$$

The critical pressure ratio is given by

$$\left.\frac{p_g}{p_0}\right|_{crit} = \left(\frac{2}{\gamma+1}\right)^{\frac{\gamma}{\gamma-1}} \tag{17}$$

Using $\gamma = 1.4$ in equations 10 to 12 results in the same equations for air-inlet valves described by Wylie et al. (1993). The equations 12 to 17 form the governing equations of the proposed model. The relation for the volume change can be derived by discretizing these equations and assuming p_g, Q_i, and Q_o to be constant in each discretized step. The change in volume between to time steps is given by

$$\Delta V = \frac{\Delta t}{\rho}\left[\sum_i \phi_{+,i} - \sum_i \phi_{-,i} + \sum_i \phi_{o,i}\right] = \left(\frac{p_n}{p_{n+1}}\right)^{\frac{1}{\gamma}} V_n - V_n \tag{18}$$

Here ΔV is the change in volume and Δt is the time step size. In this equation, the first two summations represent the volume change due to moving interfaces, the third summation represents the volume change due to flow though vents. The right-hand side represents the volume change due to changes in pressure. Each term depends on the pressure of the next time step, which is the only unknown. The equation is solved for the pressure using an adaptation of the Anderson-Björck algorithm, which is a member of the Regula Falsi family. The two summations for the moving interface can be written in terms of MoC coefficients as follows

$$\sum_i \Phi_{+,\mathrm{i}} - \sum_i \Phi_{-,\mathrm{i}} = p_g \sum_i \frac{1}{B_i} + \sum_i \frac{\mathrm{C_i}}{B_i} \tag{19}$$

Note that this is similar to the way that the MoC equations are solved at junctions. Also note that C_i is the positive or negative characteristic and depends on the topology of the pocket. Since the vents are assumed to be connected to the same atmosphere and the volume is assumed to be homogeneous, the summation over the vent flow rates can be simplified to a vent with a $c_d A$ of

$$c_d A = \sum_i (c_d A)_i \tag{20}$$

These simplified summations are independent on the pressure and are constants in the iterative solution method.

4 VOLUME TRACKING

The behavior in a pipe element is well defined; an interface can either move upwards or downwards along the pipe axis. However, at junctions an interface has to cross to different pipe elements. This may lead to splitting the air pocket into multiple smaller pockets. In heavily branched piping systems, this will occur often. Therefore, an

efficient algorithm is required to detect and split air pockets into multiple smaller pockets.
A positive interface should, per definition, always match with a downstream negative interface unless downstream the pipe element is fully drained in which case the interface matches with the downstream junction. Similarly, a negative interface should always match with an upstream positive interface or an upstream junction.
The drained part of a pipe element will be referred to as a segment. Segments may connect to one other via "drained" junction that are part of a pocket. An air pocket can be described by a set of segments such that their interfaces enclose the volume of the pocket.
If a pocket splits, then its original set of segments no longer fully connects. These situations can be identified by the following routine; pick a segment from the original pocket and add it to a list; if segment is connected to one or two junctions, then add each adjacent segment to this list (no duplicates); repeat the previous step for each newly added segment until no new segments are added to the list. If the list is not equal to the original set, then the pocket is split; a new pocket is created from the list of segments and the list removed from the original set. This is repeated until the list is equal to the original set.

5 INTERFACE-JUNCTION INTERACTION

Each time step an interface moves along the flow grid according to Equation 14. During its movement, three situations may occur; it may remain within the same grid cell; it may cross into an adjacent grid cell; and it may cross a junction.
If an interface remains within the same grid cell, then only the upstream (or downstream) grid point is affected as if it is subjected to a fixed pressure boundary.
If an interface moves into an adjacent grid cell of the same pipe element, then the flow rate of the moved-to cell is set equal to flow rate at the interface. This minimizes any inertia-based disturbances in the flow field. The liquid column's inertia will change in steps equal to the inertia of a grid cell. Therefore, the liquid column accelerates slower than other elastic models, like those of Malekpour et al. (2011) and Zhou et al. (2011, 2018). The sudden inclusion of the friction of the moved-to cell is not compensated for and will therefore lead to small pressure surges each time a cell boundary is crossed. The amplitude of this pressure surge is given by

$$\Delta p_p = f \frac{L_c}{D} \frac{\rho\, u^2}{2} \qquad 21$$

Here L_c is the grid cell's length, and u is the flow velocity in the grid cell. Compared to impact pressures and in the scope of a large pipe system this pressure is expected to become negligible. Note that the surge magnitude is proportional to the cell length. Hence, as the grid becomes denser the pressure surges vanish.
If an interface moves past a junction, then situation becomes more complex as multiple interfaces may cross the same junction in the same time step. There are two different scenarios; liquid flows into a junction that is part of an air pocket (a "drained junction"); and gas flows into a "non-drained junction" that becomes part of an air pocket. These two scenarios have been illustrated in Figure 1.

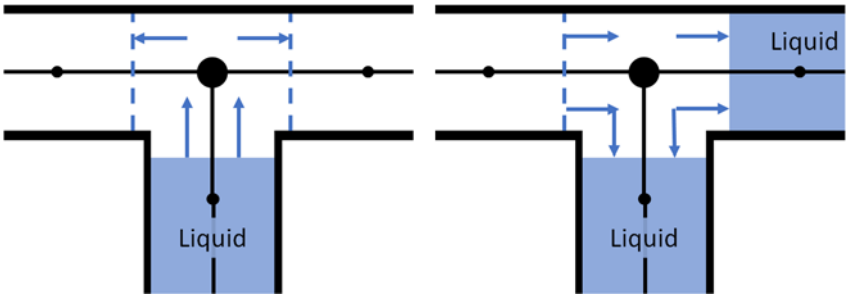

Figure 1: Illustration of two different flow scenarios at a junction. (Left) liquid flows into a junction that is part of a pocket. This causes the liquid-gas interface to split into two as indicated with the dashed-lines. (Right) gas flows from the dashed line into a junction and causes the liquid-gas interface to split into two.

A junction tracks how much swept volume of liquid or gas flows into the junction through the moving interfaces. After updating each interface, each junction has a complete balance of the amount of swept volume of either liquid or gas.
If liquid flows into a drained junction, then this junction is no longer drained. The junction is removed from the pocket's topology and the interface is moved past the junction onto each connected pipe element that is being filled. This effect may split interfaces into multiple interfaces and, consequently, split air pockets into multiple smaller air pockets. Figure 1 (Left) shows an example of an interface that splits into two interfaces. Liquid that flowed into the junction has linear momentum and, therefore, will prefer to keep moving in the same direction. The new interfaces are assigned velocities that include this effect. That is, the initial flow rates out of the junction are determined in such a way that the liquid momentum change is minimized. The initial flow rate depends on the projected inflow and outflow area

$$A_{in} = \sum_{i}^{N_{in}} A_i \min(\boldsymbol{d} \cdot \boldsymbol{r}_i, 0) \qquad 22$$

$$A_{out} = \sum_{i}^{N_{out}} A_i \min(\boldsymbol{d} \cdot \boldsymbol{r}_i, 0) \qquad 23$$

Here A_{in} and A_{out} are the projected in and outflow areas, respectively, $\boldsymbol{d}$ is the direction vector of the linear momentum, $\boldsymbol{r}_i$ and A_i are the direction vector and area of pipe element i, and N_{in} and N_{out} are the number pipe elements with flow into and out of the junction, respectively. If the outflow area is larger than the inflow area, then the linear momentum is assumed to pass undisturbed through the junction and the liquid mass flow rate associated with an interface is given by

$$\phi_i = \frac{A_i \min(\boldsymbol{d} \cdot \boldsymbol{r}_i, 0)}{A_{out}} \phi_{in} \qquad 24$$

Here ϕ_{in} is the absolute mass flow rate that flows into the junction. If the outflow area is less than the inflow area, then the flow is assumed to be restricted and part of the flow will be distributed over all the interfaces. In this case, the flow rate associated with an interface is given by

$$\phi_i = \left(\frac{A_i \min(\boldsymbol{d} \cdot \boldsymbol{r}_i, 0)}{A_{in}} + \left(1 - \frac{A_{out}}{A_{in}}\right) \frac{1}{N_{out}} \right) \phi_{in} \qquad 25$$

If gas flows into a non-drained junction, then gas begins to flow through the junction. The junction is added to the pocket's topology and a segment is created in each connected pipe element that is being drained. The initial volume of each segment is determined by the flow rate in each pipe element.

The proposed model does not support two-phase flow such as stratified flow. However, two-phase flow scenarios are possible to occur in practical use of the model. For example, two-phase flow is likely to occur when an air valve starts to take in air. Therefore, the model accounts for two-phase flow situations in a limited way so that the computed results remain realistic in may flow scenarios. A two-phase flow scenario occurs when both gas and liquid flows into a junction. If an air valve is connected to the junction, then only the difference inflow between the upstream and downstream is used to move the downstream interface while the upstream interface remains stationary. In other two-phase flow scenarios, gas is assumed to be dissolved into the liquid phase and, therefore, no longer tracked.

The proposed model has been added to an existing MoC flow solver that uses a quasi-steady wall friction model; the Darcy-Weisbach friction factor is updated each time step based on the average instantaneous flow rate in a pipe element. Note that the solver core did not require any significant changes as the flooding model is executed as an additional post-processing step after each regular MoC update.

6 MODEL ASSESSMENT

Performance, besides accuracy, was an important requirement for the flooding model. Its performance has therefore been assessed for various piping models, two of which are discussed here. The first piping model is equal to the one described by Hou et al. (2014). This model consists of a 275.2 m PVC pipeline which is rapidly filled. For this model the flooding model increases the runtime of the MoC solver (about 6 seconds) by 22% on average.
The second piping system is a cooling water system for a jet fuel tank. The pipeline branches into 20 arms around the tank wall and roof and a total of 336 sprinklers are attached to these arms. The total pipe length of this system is 907 meters. This system represents a common use case for the proposed model. The system is simulated for 20 seconds with a time step of 3.5e-4 s. After 20 seconds the system is fully flooded. For this model, the flooding model increases the runtime of the MoC solver (about 140 seconds) by 34%. This is more than the first piping model, because it involves many more gas pockets that move through the piping system. Although an increase of 34% in the execution time is significant, it can be deemed fairly modest when compared to alternative two-phase flow solutions.
The accuracy of the proposed model has been assessed by comparing its results with those published by Zhou (2002, 2011, 2018) and Hou (2014).

Zhou et al. (2011) investigated the influence of entrapped air pockets on hydraulic transients. Their experimental setup consists of a 4.445-meter pipe that has an entrapped air pocket at atmospheric pressure on one end and a tank on the other. The rapid opening of a ball valve causes a sudden liquid flow together with the expulsion of the entrapped air. They compared their proposed elastic model with experimental

results. Their experiment has been modelled with our proposed model. Here we assume the same properties as they used in their model. Their results and the results of our proposed model are depicted in Figure 2. Our model follows theirs closely for air fractions f_a of less than 1%. For air fractions between 1% and 6% our model, like the one from Zhou, predicts a pressure that is higher than the measurements. For larger air fractions our model is in more agreement with the experiments. The last section piping in the experimental setup is horizontal. For small air fractions, the assumption that the interface is perpendicular to the pipe axis is invalid as the liquid-air interface is parallel to the pipe axis. This may explain the difference in pressure surge at small air fractions.

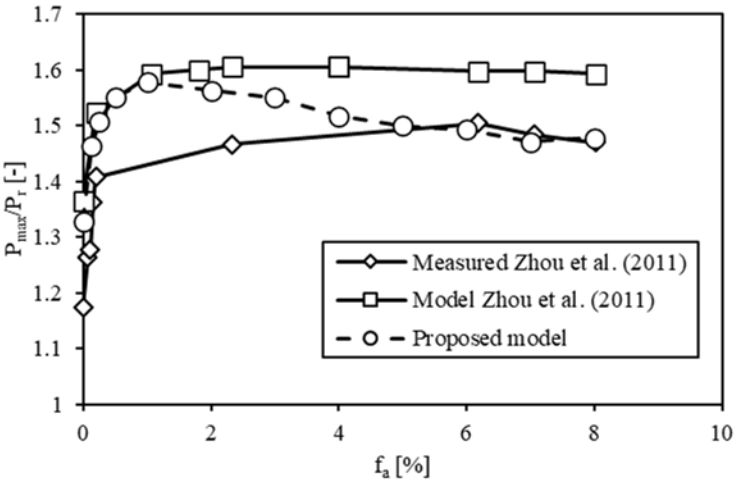

Figure 2: Maximum relative absolute pressure as function of initial air fraction for (diamond) measurements of Zhou et al. (2011), (square) virtual-plug model by Zhou et al. (2011), and (circle) our proposed model. Here $H_{max}$is the absolute maximum pressure and H_r is the absolute initial pressure supplied by the tank. In this case H_r is 0.16 MPa (abs.).

Zhou et al. (2018) did an extensive experimental study on the effect of air expulsion though an orifice. Their experimental setup consists of a pressure vessel connected to an 8.862-meter horizontal pipe that end in a bend upwards. In their study an air pocket in the vertical pipe is expelled from an orifice at the top of the vertical pipe. They present results for three pressures, seven initial air volumes, and 20 orifice sizes. The measured wave speed in the pipeline without air is 850 m/s.

Their experimental setup has been simulated with our proposed model. The pressure vessel has been represented with a fixed pressure boundary condition. The relation between the maximum pressure and relative orifice size is shown in Figure 3. Zhou et al. (2018) identified two types of behaviours. Type 1 identifies a long-period of pressure oscillations and no significant water hammer impact pressure. Type 2 are associated with short oscillations and a higher water hammer impact pressure. The two types are also visible with the proposed model. The cushioning effect of the air pocket reduces the maximum pressure up to a d/D of 0.05. The cushioning effect diminishes for large d/D and the maximum pressure is dominated by the impacting water hammer. The proposed model shows that the maximum pressure increases with increasing air length, see Figure 4. The proposed model follows the same trend as

the experimental results up to an air pocket length of 3.39%. Beyond that length the results to deviate, however. The experiments show a decrease in maximum pressure after an air pocket length of 3.39%. Zhou et al. (2018) concluded that when the initial air pocket is larger than a critical length (3.39% in their experiments), then the filling velocity is slowed and, consequentially, the maximum pressure is reduced. The proposed model does not result in the same trend; the maximum observed pressure keeps increasing. The reason for this deviation is not known.

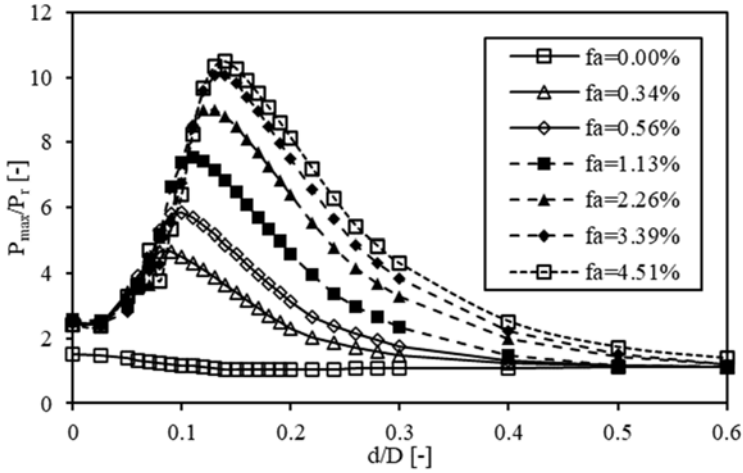

Figure 3: Relation between maximum absolute pressure and relative orifice size d/D for different air fractions f_a. Here P_r is 0.26 MPa (abs.).

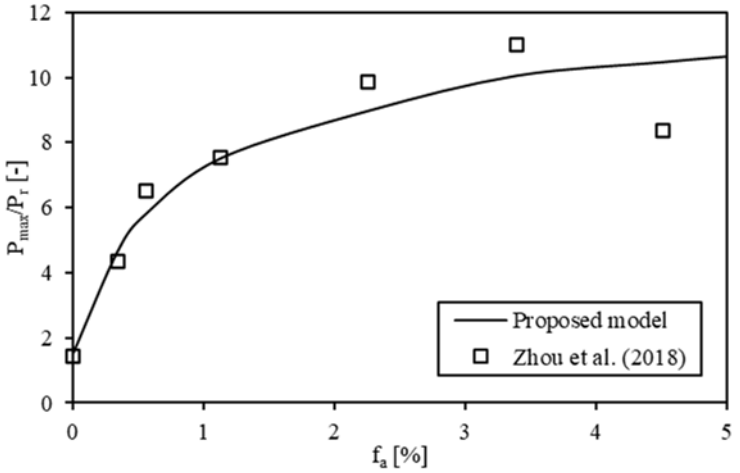

Figure 4: Maximum pressure as function of initial air pocket size for (solid) proposed model and (square) Zhou et al. (2018) experimental results. Here P_r is 0.26 MPa (abs.).

Zhou et al. (2002) did experiments with a horizontal configuration of a pipe with entrapped air and an orifice for air release. In their paper they derived a rigid body model. Their model is in good agreement with their experimental results. They

measured the wave speed during their experiments and used those wave speeds in their model. Zhou et al. (2002) specifies that the wave speed is in the range of 200 m/s to 1400 m/s. For our experiments, a wave speed of 400 m/s, 1000 m/s, and 1400 m/s are used for 4.8%, 50%, and 80% initial liquid fractions, respectively. This resulted in more or less the same maximum pressures.

Figure 5 show the results of proposed model on the experimental setup from Zhou et al. (2002) with an upstream pressure of 343 kPa. For an initial liquid fraction of 80%, our model predicts local minima and maxima in the transition regime ($0.05 < d/D < 0.2$). These minima and maxima are a result of the timing of fully expulsion of air from the pipe. The pressure of the entrapped air increases during the rapid filling, slowing down the liquid column. For small orifice diameters, the inertia of the liquid column causes the velocity to oscillate; see Figure 5. Consequently, the exact moment when all air has been expelled determines the velocity of impact, and therefore the maximum pressure. As a consequence, the maximum pressure oscillates as the orifice diameter increases.
This oscillation is less significant for the other liquid fractions as it is dampened by friction. Since the liquid column travels a longer distance, the oscillation will be dampened more. This oscillation is not present in the experimental and numerical results of Zhou et al. (2002).

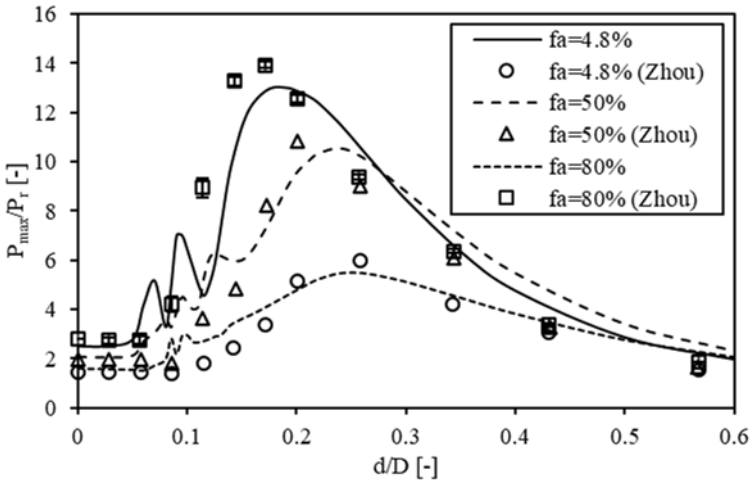

Figure 5: Maximum relative absolute pressure as function of relative orifice size for (lines) proposed model and (markers) experimental results Zhou et al. (2002). The upstream pressure P_r is 0.44 MPa (abs.).

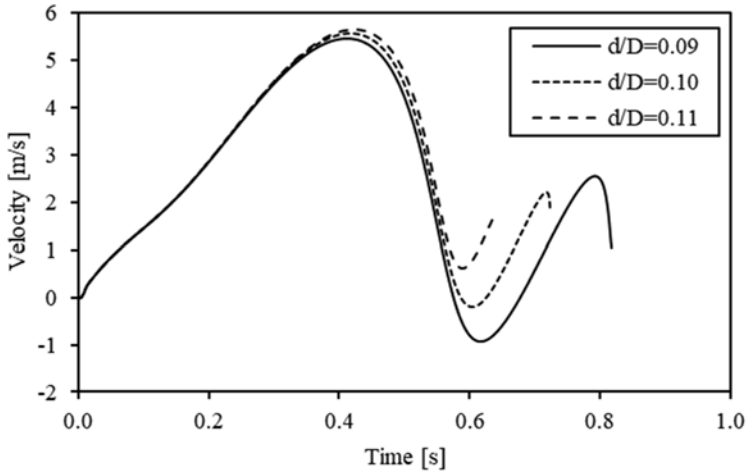

Figure 6: Front velocity as function of time for three different relative orifice sizes at a relative liquid fraction of 80%. The liquid column reaches the orifice at different velocities depending on the phase in the oscillation.

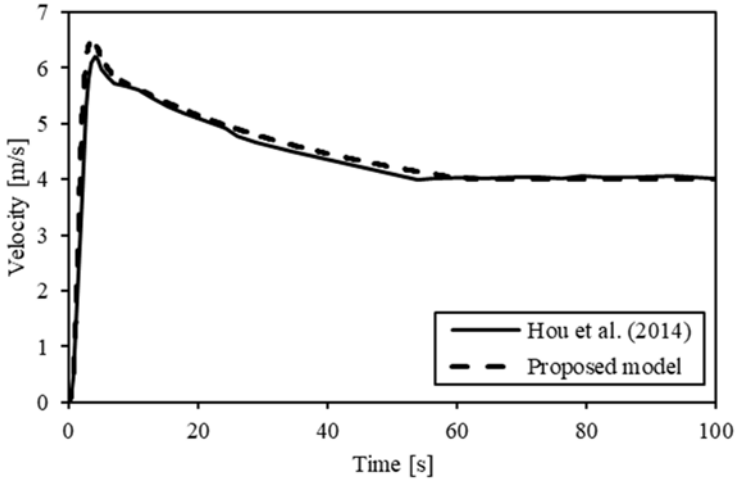

Figure 7: Front velocity as function of time for the experimental setup of Hou et al. (2014). The results of Hou et al. (2014) are denoted with a solid line and the proposed model with a dashed line.

Hou et al. (2014) investigated rapid filling of a larger pipeline system. Their experimental pipeline consists of a 275.2-meter-long PVC pipe and some steel piping. The PVC pipe was initially empty and filled rapidly. However, they noted that there is entrapped air in some of the steel piping. In our model this volume is estimated to be 0.53 m^3 and is modelled as a surge vessel as described by Wylie et al. (1993). In our model the friction is set to match the steady state results obtained by Hou et al. (2014). The comparison between the measured front velocity and the proposed model is shown in Figure 7. The proposed model is consistent with the front velocity measurements. It should be noted that entrapped air pocket of 0.53 m^3

causes the maximum velocity and the oscillation in the first 10 seconds. Without this extra volume the maximum velocity is lower and is the initial curve less steep.

7 CONCLUSIONS

The numerical model for modelling rapid filling of pipelines presented here simplifies the elastic models for rapid filling as proposed by Malekpour et al. (2011) and Zhou et al. (2018) to trade off accuracy for performance and implementation simplicity. In the proposed model, special attention is given to volume tracking and the interaction between junctions and air pockets. The results show that the proposed model increases the execution time of an efficient MoC solver with 34% when it is used to simulate the filling of a heavily branched piping system.
The proposed model compares reasonably well with experiments and numerical results found in literature despite of the reduction in accuracy of the proposed model. These experiments include situations of small and large air pockets. Therefore, it is reasonable to assume if the proposed model can predict these situations, then the proposed model can predict the impact pressure surges in larger and more complex piping systems during rapid filling.

REFERENCES

(1) Q. Hou, A. S. Tijsseling, J. Laanearu, I. Annus, T. Koppel, A. Bergant, S. Vučkovic, A. Anderson and J. M. C. van 't Westende, *Experimental Investigation on Rapid Filling of a Large-Scale Pipeline*, Journal of Hydraulic Engineering, vol. 140, no. 11, pp. 04014053, 2014.

(2) L. Li, D. Z. Zhu and B. Huang, *Analysis of Pressure Transient Following Rapid Filling of a Vented Horizontal Pipe*, Water, vol. 10, pp. 1698, 2018.

(3) C. P. Liou and W. A. Hunt, *Filling of pipelines with undulating elevation profiles*, Journal of Hydraulic Engineering, vol. 122, no. 10, pp. 534-539, 1996.

(4) A. Malekpour and B. W. Karney, *Rapid Filling Analysis of Pipelines with Undulating*, ISRN Applied Mathematics, 2011.

(5) L. Wang, F. Wang, B. W. Karney, A. Malekpour and Z. Wang, *Influence of velocity head on filling transients in a branched pipeline*, Engineering Computations, vol. 35, 2018.

(6) E. B. Wylie and V. L. Streeter, *Fluid Transients in Systems*, Upper Saddle River: Prentice-Hall, Inc., 1993.

(7) F. Zhou, F. E. Hicks and P. M. Steffler, *Transient Flow in a Rapidly Filling Horizontal Pipe*, Journal of Hydraulic Engineering, vol. 128, 2002.

(8) L. Zhou, D. Liu, B. Karney and Q. Zhang, *Influence of Entrapped Air Pockets on Hydraulic Transients in Water Pipelines*, Journal of Hydraulic Engineering, vol. 137, pp. 1686-1692, 2011.

(9) L. Zhou, T. Pan, H. Wang, D. Liu and P. Wang, *Rapid air expulsion through an orifice in a vertical water pipe*, Journal of Hydraulic Research, vol. 57, pp. 1-11, 2018.

(10) Federal emergency management agency, Handbook of chemical hazard analysis procedures, 1989, p. Appendix B.